Controlled excitation of selected regions inside dielectric media

J. R. Csesznegi, B. K. Clark, and R. Grobe
Intense Laser Physics Theory Unit and Department of Physics, Illinois State University, Normal, Illinois 61790-4560
(Received 5 December 1997)

We propose an optical scheme to control the degree of excitation of spatially localized regions inside an absorbing three-level medium using two suitably delayed laser pulses. Only selected localized regions inside the medium are changed by the pulses, the remaining medium remains unchanged in its ground state. We present an approximate but analytical theory of the coupled Liouville and Maxwell equations and propose an experimental verification of this control excitation scheme for potassium vapor. [S1050-2947(98)02606-7]

PACS number(s): 42.65.Hw, 42.65.Re

I. INTRODUCTION

There has been some growing interest in manipulating the quantum-mechanical state of dielectric materials using laser light. The challenge of coherent control is to exploit either (a) tailor-made waves to drive matter to a desired state or (b) certain properties of matter to design wave forms. In the last decade exciting experimental and theoretical progress was made in both categories.

A commonly used laser technique of driving an atom into a desired excited state involves the coherent interaction with a laser field of specified pulse area. Other methods to efficiently excite selected states require a time-dependent detuning (chirped pulses). Recently, the application of two or several laser pulses has been proposed to excite selected atomic or molecular states with high efficiency. A good example is the experimental work of Bergmann and co-workers [1], in which a sequence of two appropriately delayed resonant laser pulses is used to transfer population into a higher lying state.

The possibility of controlling the quantum-mechanical degree of coherence of an atom or a molecule has also led to some progress in understanding the optical properties of dielectric media. Harris's pioneering work [2] experimentally demonstrated that the transmission properties of an atomic medium can be changed significantly if a second strong laser field is applied. The theoretical analysis of the fully coupled interaction of two laser fields with a three-level system is very challenging. For a medium that is initially in the ground state, soliton wave forms have been predicted [3] and recently the cloning of wave forms using two-photon coherences [4] has been proposed. Analytical solutions and a better understanding is possible in the regime in which the medium's response to the fields is temporally adiabatic [5]. Here it is possible to combine the principles of the dark-state dynamics, counterintuitive pulse sequencing, and two-photon adiabaticity to derive coupled wave equations which allow for fully analytical solutions. Novel solitonic wave forms called ''adiabatons'' have been predicted using this approach [6,7]. In 1995 an experimental observation of adiabatons [8] was reported.

In almost all investigations, each of the atoms or molecules of the medium was either the ground state or a coherent superposition [9–13] of states. Recently, the remarkable optical properties of a novel medium have been investigated [14], in which the degree of excitation does depend on the position. In this work we will discuss how a sequence of appropriately delayed laser pulses can be used to produce these spatially dependent excitations in a laboratory. We will demonstrate that it is possible to use the laser pulses to control the state of specified spatial regions inside an absorbing medium without affecting the remaining domains. This situation can be achieved if the laser fields are nearly resonant with the same upper atomic state and are injected into the medium in the counterintuitive order. The two pulses interact fully dynamically with the medium and at a predetermined propagation depth one pulse will decay to excite the material. This coherent interaction can even be used to control not only the final population in selected states, but also to generate specific phase relations between the corresponding state amplitudes.

Our paper is organized as follows. We first review the essential equations which govern the interaction of a medium of three-level atoms or molecules with two nearly resonant laser fields. This section will also introduce the relevant parameters. In the third section we will provide a simplified analytical theory based on temporal adiabaticity and compare our analytical results with those obtained from the numerical integration of the full set of equations. In the fourth section we discuss the relevant parameters to control the degree of excitations in a potassium vapor. Finally, we conclude with a brief discussion and a very speculative outlook on possible applications.

II. BASIC EQUATIONS AND PARAMETERS

In Fig. 1 we have sketched the relevant parameters for the medium as well as the relevant time scales for the simplest case of two incoming laser pulses. We denote with L the total length of the material, D_1 is the penetration depth at which we would like to excite the medium into a specified metastable state, and the thickness of this metastable layer is denoted by D_2-D_1. The time when the first laser field is injected into the medium (at $z=0$) is denoted by $t=0$. The two input laser pulses can be characterized by their temporal duration denoted by $t_{\rm off}-t_{\rm on}$ and T_b and by their mutual delay at turn on $t_{\rm on}$. The choice of the penetration depths D_1 and D_2 determines the values for $t_{\rm on}$, $t_{\rm off}$, and T_b. The final degree of the excitation as well as its spatial profile is controlled by the laser intensities and the pulse shapes at input.

We assume that the optical medium is characterized by

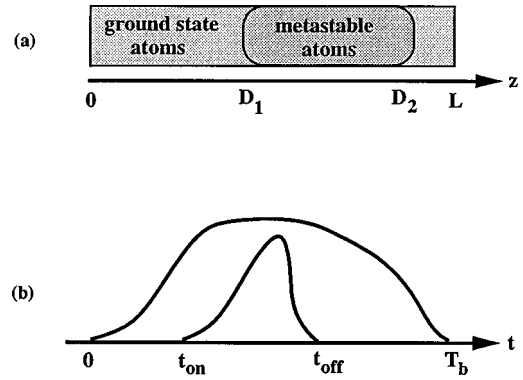

FIG. 1. The relevant parameters. (a) The medium's length scales D_1, D_2, and L. (b) The time scales for the two input pulses at the entry surface of the medium T_b, $t_{\rm on}$, and $t_{\rm off}$.

three atomic or molecular energy levels. We describe the state of each atom or molecule by nine matrix elements of the density operator ρ_{ij}. Each matrix element is a function of time and space. The ground state is denoted by $|1\rangle$ and the metastable state which we want to excite is denoted by $|3\rangle$. We assume that both states are dipole coupled to a common upper state $|2\rangle$. For the numerical simulations discussed in Sec. III, we have assumed various kinds of irreversible mechanisms that are relevant to a vapor of potassium molecules, for which we propose an experiment.

In Fig. 2 we show a typical energy scheme of a three-level λ system with the most relevant couplings. The parameters A_{21} and A_{23} correspond to the spontaneous emission from the upper level into states $|1\rangle$ and $|3\rangle$, and we have also included the dipole dephasing between levels $|1\rangle$ and $|2\rangle$, $|2\rangle$ and $|3\rangle$, and $|1\rangle$ and $|3\rangle$ with the decay rates γ_{12}, γ_{23}, and γ_{13}, respectively. An irreversible decay rate of the upper state due to ionization or coupling to other levels that are not included in the model is denoted by Γ. We have also allowed for detunings $\Delta_a=(E_2-E_1)/\hbar-\omega_a$, and $\Delta_b=(E_2-E_3)/\hbar-\omega_b$, where E_i are the energies of the relevant levels and $\omega_{a,b}$ denote the respective laser frequencies.

For simplicity we have transformed the space and time variables to a coordinate system moving with the speed of light c: $\tau=t-z/c$, where τ denotes a delayed time. The equations for the density matrix elements take the following

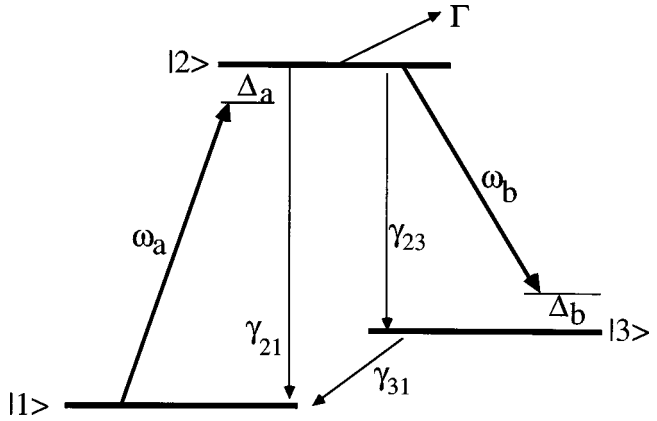

FIG. 2. Energy level scheme of a three-level λ atom or molecule.

form in the rotating-wave approximation:

$$i\frac{\partial}{\partial\tau}\rho_{11}(z,\tau)=-\frac{1}{2}(\Omega_a^*\rho_{12}-\Omega_a\rho_{21})+iA_{21}\rho_{22}, \tag{2.1a}$$

$$i\frac{\partial}{\partial\tau}\rho_{22}(z,\tau)=-\frac{1}{2}(\Omega_a\rho_{21}+\Omega_b\rho_{23}-\Omega_a^*\rho_{12}+\Omega_b^*\rho_{32}) -i(A_{21}+A_{23}+2\Gamma)\rho_{22}, \tag{2.1b}$$

$$i\frac{\partial}{\partial\tau}\rho_{33}(z,\tau)=-\frac{1}{2}(\Omega_b^*\rho_{32}-\Omega_b\rho_{23})+iA_{23}\rho_{22}, \tag{2.1c}$$

$$i\frac{\partial}{\partial\tau}\rho_{21}(z,\tau)=\frac{1}{2}[\Omega_a^*(\rho_{11}-\rho_{22})+\Omega_b^*\rho_{31}] -i(\beta_{21}+\Gamma-i\Delta_a)\rho_{21}, \tag{2.1d}$$

$$i\frac{\partial}{\partial\tau}\rho_{23}(z,\tau)=\frac{1}{2}[\Omega_b^*(\rho_{33}-\rho_{22})+(\Omega_a^*\rho_{13})] -i(\beta_{23}+\Gamma-i\Delta_b)\rho_{23}, \tag{2.1e}$$

$$i\frac{\partial}{\partial\tau}\rho_{31}(z,\tau)=\frac{1}{2}[\Omega_b\rho_{21}-\Omega_a^*\rho_{32})]-(i\gamma_{31}+\Delta_b-\Delta_a)\rho_{31}. \tag{2.1f}$$

The phenomenological constants [15] which account for damping have been defined as $\beta_{21}\equiv 0.5(A_{21}+A_{23})+\gamma_{21}$ and $\beta_{23}\equiv 0.5(A_{21}+A_{32})+\gamma_{23}$.

The laser field is a sum of two laser pulses

$$E(z,t)=E_a(z,t)\exp\{i\omega_a(t-z/c)\} +E_b(z,t)\exp\{i\omega_b(t-z/c)\}+\text{c.c.}, \tag{2.2}$$

with the two near resonant optical frequencies ω_a and ω_b. The two components can have sufficiently different frequencies such that each of them is coupled only to one transition, 1-2 (for E_a) and 2-3 (for E_b). We use the slowly varying envelope approximation so that the temporal and spatial evolution of each field amplitude is governed by a reduced wave equation. We neglect transverse propagation effects. The notation is simplified if we replace the electric field amplitudes by Rabi frequencies via $\Omega_a\equiv 2d_aE_a/\hbar$ and $\Omega_b\equiv 2d_bE_b/\hbar$, where d is the dipole moment between the relevant levels.

$$\frac{\partial}{\partial z}\Omega_a(z,\tau)=i\mu_a\int d\Delta_a\rho_{12}(z,\tau)g_a(\Delta_a), \tag{2.3a}$$

$$\frac{\partial}{\partial z}\Omega_b(z,\tau)=i\mu_b\int d\Delta_b\rho_{32}(z,\tau)g_b(\Delta_b). \tag{2.3b}$$

The coupling coefficients $\mu_{a,b}$ are related to the number density of atoms $\mathcal{N}$ via $\mu_{a,b}\equiv\mathcal{N}d_{a,b}^2\omega_{a,b}/\varepsilon_0\hbar c$. The function $g(\Delta)$ is the inhomogeneous linewidth of the medium due to the velocity distribution of the atoms in the vapor.

In order to test the regime of validity of our analytical theory presented below, we have solved the fully coupled Liouville-Maxwell equations (2.1) and (2.3) on a spatial-time

grid. For the total interaction time, we have used about 20 000 grid points and, for the spatial grid, 40 000. The coupled equations have been solved using a standard Runge-Kutta fourth-order algorithm for the integration in time and a simple Euler algorithm for the integration in space. To test the numerical accuracy we reduced the grid points in each direction by a factor of 2 and found that the results were unchanged.

III. THEORETICAL ANALYSIS OF THE SPATIAL EXCITATION PROCESS

A. Analytical theory based on adiabaticity

The physics of the excitation process can be qualitatively described as follows. One long and one short pulse are injected into a medium that is in its ground state. The long pulse, Ω_b, is injected into the medium first as shown in Fig. 1(b). The short pulse, Ω_a, exchanges its energy with the medium when the front edge of the pulse is absorbed by the medium and the same amount of energy is then transferred back into the trailing edge of the same pulse. The medium left behind is in the ground state. This exchange mechanism requires the presence of both fields and effectively slows down pulse Ω_a. The larger is the Ω_a pulse intensity, the more the Ω_a pulse velocity is reduced. This means that its trailing edge comes closer to the trailing edge of Ω_b pulse that moves with the speed c. The trailing edge of Ω_b is not slowed down as the medium is left behind in the ground state, because Ω_b does not couple directly to the ground state.

After a characteristic propagation distance, the (fast) trailing edge of Ω_b has caught up with the edge of Ω_a. As Ω_b is turned off, the medium cannot return the energy back into pulse Ω_a and Ω_a begins to decay. Part of its energy remains in the medium and part of it is converted to the energy of pulse Ω_b. When pulse Ω_a has decayed a layer of excitation is left behind.

Below we will derive analytical formulas for the degree of energy conversion, the spatial profiles of the layers of excitation, and the requirements on the laser pulses to produce specific spatial excitation patterns. Our theory is based on the theory of adiabatons as first introduced in Ref. [6]. In the adiabatic regime, the time evolution follows one eigenvector, the so-called trapped state [16]. This state relates the state populations of the atom to the Rabi frequencies: $\rho_{11}=|\Omega_b/\Omega|^2$ and $\rho_{33}=|\Omega_a/\Omega|^2$, where the two-photon Rabi frequency is denoted by $\Omega^2\equiv|\Omega_a|^2+|\Omega_b|^2$. In order to exclusively excite the trapped state, the laser field Ω_b that is coupled to the initially ''empty'' transition (2-3) has to be turned on before the pulse Ω_a, which couples to the initially populated ground state [17]. A generalization to ''hot'' media with a thermally populated state $|3\rangle$ is discussed in Sec. IV. In order to guarantee that the other eigenstates remain practically decoupled from the dynamics, the two Rabi frequencies have to satisfy the well-known condition [18]

$$\left|\Omega_a\frac{\partial}{\partial\tau}\Omega_b-\Omega_b\frac{\partial}{\partial\tau}\Omega_a\right|\ll\sqrt{[\Omega_a^2+\Omega_b^2]^3}. \tag{3.1}$$

Inequality (3.1) is more easily satisfied for stronger fields. If this condition of temporal adiabaticity [5] holds the final state of the medium after the two pulses have passed is determined by the following relation:

$$G(z)\equiv\rho_{33}(z,\tau\to\infty)=|\Omega_a(z,\tau\to\infty)/\Omega(z,\tau\to\infty)|^2. \tag{3.2}$$

The limit $\tau\to\infty$ is meant in a physical (not mathematical) sense. It is clear that if both pulses (or the corresponding areas) are too small, the actual population in state $|3\rangle$ cannot be changed.

The central goal of this work is to find the temporal characteristics of two input pulses that can generate the final state of the medium in accordance to a chosen excitation function $G(z)$. The difficulty in evaluating the expression Eq. (3.2) arises because both pulses interact nonperturbatively with the material and change their shapes as they propagate through the medium. In the adiabatic regime, however, the temporal and spatial evolution of both laser pulses can be found analytically. The evolution of the two pulses is characterized by the following set of nonlinearly coupled wave equations [6]:

$$\frac{\partial}{\partial z}\Omega_a=-\frac{2\mu_a}{\Omega}\frac{\partial}{\partial\tau}\frac{\Omega_a}{\Omega}, \tag{3.3a}$$

$$\frac{\partial}{\partial z}\Omega_b=-\frac{2\mu_b}{\Omega}\frac{\partial}{\partial\tau}\frac{\Omega_b}{\Omega}. \tag{3.3b}$$

As the decay of pulse Ω_a is important with respect to the final excitation of the medium, we will first discuss how the number of photons and the energy of the pulse Ω_a change with increasing propagation distance. The total electromagnetic field energy per unit area of each pulse that passes through position z can be obtained directly from the Rabi frequency via $w_a\equiv\varepsilon_0 c\hbar^2\int d\tau|\Omega_a(z,\tau)|^2/(2d_a^2)$. If we multiply both sides of Eq. (3.3a) with Ω_a and integrate with respect to τ, we find the following relation between the final population in the excited state and the spatial variation of the time-integrated squared Rabi frequency.

$$\frac{\partial}{\partial z}\frac{1}{2\mu_a}\int_0^\infty d\tau|\Omega_a(z,\tau)|^2=-\rho_{33}(z,\tau=\infty), \tag{3.4}$$

where we have used the initial condition $\rho_{33}(z,\tau=0)=0$ and the trapped-state relation $\rho_{33}=|\Omega_a/\Omega|^2$. The integral $(1/2\mu_a)\int_0^\infty d\tau|\Omega_a(z,\tau)|^2=[w_a/(\hbar\omega_a)]/\mathcal{N}$ has a direct interpretation: it is the ratio of the total number of the photons passing through z and the number of atoms per unit length. This ratio does not depend on the dipole moment. The ''conservation'' law of Eq. (3.4) shows that the field cannot lose any energy at those locations z at which the medium is left behind in the ground state $[\rho_{33}(z,\tau=\infty)=0]$. For the simple situation sketched in Fig. 1 this is required for short propagation distances $z<D_1$ and also for $z>D_2$. For short distances $z<D_1$, the (fast) trailing edge of Ω_b cannot reach the (slow) trailing edge of Ω_a. As both pulses interact strongly even for $z<D_1$, the conservation law does not guarantee shape-invariant propagation. If we integrate Eq. (3.4) over the distance z and multiply with $\mathcal{N}$, we obtain

$$\mathcal{N}\frac{1}{2\mu_a}\int_0^\infty d\tau|\Omega_a(z=0,\tau)|^2-\mathcal{N}\frac{1}{2\mu_a}\int_0^\infty d\tau|\Omega_a(z=L,\tau)|^2$$

$$=\mathcal{N}\int_0^L dz\rho_{33}(z,\tau=\infty). \tag{3.5}$$

This relation illustrates how the electromagnetic field ''energy'' of the pulse can be converted into the atomic excitation energy. Each term on the left-hand side is the total number of photons in the pulse that has passed through position z. The difference between the two terms is the number of photons that were used to excite the atoms. The right-hand side is the number of metastable atoms in the entire medium per unit area.

Let us now solve the adiabatic wave equations, Eqs. (3.3), and present the solution for $\Omega_a(z=L,\tau)$. Although these equations are coupled through the two-photon field $\Omega^2 \equiv|\Omega_a|^2+|\Omega_b|^2$, the spatial and temporal evolution of the fields can be expressed analytically for any arbitrary initial fields. It is easy to see that these equations can be written in a fully integrable form if we assume equal oscillator strength for both transitions ($\mu_a=\mu_b$) and introduce the nonlinear variable $X(\tau)$:

$$X(\tau)\equiv\frac{1}{2\mu}\int^\tau d\tau'|\Omega(z=0,\tau')|^2. \tag{3.6}$$

The analytical solution of Eq. (3.3) can be expressed directly as a function of the (arbitrary) input laser pulses at $z=0$:

$$\Omega_{a,b}(z,\tau)=\frac{\Omega_{a,b}[z=0,X^{-1}(X(\tau)-z)]}{\Omega[z=0,X^{-1}(X(\tau)-z)]}\,\Omega(z=0,\tau), \tag{3.7}$$

where $X^{-1}(\ )$ denotes the inverse function to the integral $X(\tau)$. If the total Rabi frequency $\Omega(z=0,\tau)$ happens to be time independent after a suitable turn on, the field $\Omega_a(z,\tau)$ is only a function of $X(\tau)-z$ and can propagate with invariant shape after a characteristic propagation distance. These shape-invariant solutions are called adiabatons. Adiabatons are solitonlike pulse pairs that are formed by an absorbing medium and can propagate in a medium without significant loss. References [6,7] have shown that Eq. (3.7) describes the spatial and temporal evolution with a remarkable precision, if dissipative mechanisms that are not directly related to state $|2\rangle$ are negligible and inequality (3.1) is satisfied.

For the present work we do not require the formation of any shape-invariant solutions. If the medium's total length L exceeds $X(T_b)\equiv Z$, the fields can propagate a sufficient distance such that part of the energy of the pulse Ω_a can be converted into that of the other pulse Ω_b. The temporal shapes of the output pulses follow immediately from the solution Eq. (3.7), using $X^{-1}(0)=0$ and $\Omega_a(z=0,\ \tau=0)=0$. We obtain interesting pulse shapes for $z>Z$:

$$\Omega_a(z>Z,\tau)=0, \tag{3.8a}$$

$$\Omega_b(z>Z,\tau)=\sqrt{[\Omega_a(z=0,\tau)^2+\Omega_b(z=0,\tau)^2]}. \tag{3.8b}$$

It is interesting to note that, although the field Ω_b experiences some significant reshaping as it propagates through the medium, its output shape is practically identical to its shape at input with the only exception of those times τ where both pulses overlapped at input. It is also remarkable that, even though the entire temporal and spatial evolution depends on μ, the final output pulse shape does not.

The final state of the fields can be used to complete our energy analysis for the excitation process. Recalling the definition of the electromagnetic field energy per unit area that has passed through a position z, $w_{a,b}\equiv\varepsilon_0 c\hbar^2\int d\tau|\Omega_{a,b}|^2/(2d_a^2)$, and using the relations Eq. (3.8) we find for the electromagnetic field energy w_b at output ($z>Z$)

$$w_b(z>Z)=w_b(z=0)+\frac{\omega_b}{\omega_a}\,w_a(z=0). \tag{3.9}$$

In other words, a fraction of the energy of the input pulse Ω_a is used to increase the energy of the field Ω_b at output by the amount $(\omega_b/\omega_a)w_a(z=0)$. If we assume that the ground state of the medium has zero energy ($E_1=0$), then the total excitation energy contained in the medium per unit area is $W_{\rm med}(\tau)\equiv\mathcal{N}\hbar(\omega_a-\omega_b)\int dz\rho_{33}(z,\tau)$. It follows directly from relation Eq. (3.5) that the remaining fraction of the input field energy $[1-(\omega_b/\omega_a)]w_a(z=0)$ is converted into the excitation energy of the medium according to

$$W_{\rm med}(\tau=\infty)=\mathcal{N}\hbar(\omega_a-\omega_b)\int dz\rho_{33}(z,\tau=\infty)$$

$$=(1-\omega_b/\omega_a)w_a(z=0). \tag{3.10}$$

As a next step we investigate how the medium's excitation evolves under the two pulses. Assuming that the medium remains in the trapped state throughout the evolution we find from Eq. (3.7)

$$\rho_{33}(z,\tau)=\left|\frac{\Omega_a(z=0,X^{-1}(X(\tau)-z))}{\Omega(z=0,X^{-1}(X(\tau)-z))}\right|^2. \tag{3.11}$$

This expression shows that, after the medium has been brought into its metastable state, the excitations can travel through the medium with a velocity $-(\partial/\partial\tau)\rho_{33}/(\partial/\partial z)\rho_{33}=\Omega^2/2\mu$ in the moving coordinate frame or, equivalently, with a velocity $-(\partial/\partial t)\rho_{33}/(\partial/\partial z)\rho_{33}=2\mu c/(2\mu+c\Omega^2)$ in the laboratory frame.

The main goal of the present work is to investigate how two input pulses can be employed to excite the medium at a specified depth. After both pulses have passed through the medium, the final spatial distribution of the population in the metastable state $|3\rangle$ is given by

$$\rho_{33}(z,\tau\to\infty)\equiv G(z)=\left|\frac{\Omega_a(z=0,X^{-1}(Z-z))}{\Omega(z=0,X^{-1}(Z-z))}\right|^2. \tag{3.12}$$

If we assume that the input pulse Ω_a is practically nonzero for $t_{\rm on}\leqslant t\leqslant t_{\rm off}$ as shown in Fig. 1, then it follows that the final population in state $|3\rangle$ $\rho_{33}(z,\tau\to\infty)$ is nonzero at regions z,

$$D_1 \equiv Z - X(t_{\rm off}) \geqslant z \geqslant Z - X(t_{\rm on}) \equiv D_2 . \qquad (3.13)$$

This relation defines implicitly the required turn-on and turn-off parameters as a function of the chosen lengths D_1 and D_2.

Unfortunately, Eq. (3.12) is an implicit relation to determine the two laser pulse shapes from a chosen function $G(z)$. To find the characteristics of the input laser pulses as a direct function of arbitrary spatial excitation profiles $G(z)$ is a quite interesting mathematical problem, perhaps it is not even solvable in full generality unless numerical techniques are applied.

B. Two analytically solvable cases

It might be illustrative, however, to examine two special cases of input pulse shapes, for which relation Eq. (3.12) can be inverted. In the first one, we restrict the envelopes of both pulses to take constant amplitudes: $\Omega_a(z=0,\tau)=A$ for $t_{\rm on} \leqslant \tau \leqslant t_{\rm off}$ and $\Omega_b(z=0,\tau)=B$ for $0 \leqslant \tau \leqslant T_b$. For this case we find for the pulse delay parameters

$$t_{\rm on} = T_b - \frac{2\mu}{A^2+B^2} D_2 - \frac{A^2}{B^2} \frac{2\mu}{A^2+B^2} D_1 , \qquad (3.14a)$$

$$t_{\rm off} = T_b - \frac{2\mu}{B^2} D_1 . \qquad (3.14b)$$

The spatial excitation distribution $G(z)$ would be equal to $A^2/(A^2+B^2)$ for $D_1 \leqslant z \leqslant D_2$ and zero outside. The required duration of the input pulse Ω_a is $t_{\rm off}-t_{\rm on}=[2\mu/(A^2+B^2)](D_2-D_1)$. Note that in this example it is impossible to transfer all the population into the metastable state, if $B \ll A$.

For the second analytical example, it is possible to express both pulses directly as a function of an arbitrary excitation profile $G(z)$. Let us assume that both input pulses have ''antimatched'' envelopes such that $\Omega_a(z=0,\tau)^2 + \Omega_b(z=0,\tau)^2 \equiv B^2$ is a square pulse for $0<\tau<T_b$ and zero otherwise. This, of course, does not necessarily imply that Ω_a and Ω_b are constant. In this case, the characteristic propagation distance is $Z=(B^2/2\mu)T_b$ and the integral $X(\tau)=(B^2/2\mu)[\tau-(\tau-T_b)\vartheta(\tau-T_b)]$, where $\vartheta(\,)$ is the Heaviside unit step function. Its inverse function $X^{-1}(x) = (2\mu/B^2)x$ for $0 \leqslant x < Z$ and it has a singularity at $x=Z$. If we insert this into Eq. (3.12) and solve for $\Omega_{a,b}(z=0,\tau)$, we obtain the shapes of the input pulses as a function of the given excitation profile $G(z)$:

$$\Omega_a(z=0,\tau) = B\left[G\left(z = \frac{B^2}{2\mu}(T_b-\tau) \right) \right]^{1/2}, \qquad (3.15a)$$

$$\Omega_b(z=0,z\tau) = B\left[1 - G\left(z = \frac{B^2}{2\mu}(T_b-\tau) \right) \right]^{1/2}. \qquad (3.15b)$$

In this case, the required input pulse shape for Ω_a^2 is just a mirror symmetric replica of the spatial excitation profile. Let us assume $G(z)$ is practically nonzero for the distance $D_1 < z < D_2$. It follows immediately that the total pulse duration T_b has to be sufficiently long for a given pulse energy, $T_b > (2\mu/B^2)D_2$. The deeper the layer to be excited inside the medium is, the longer the pulses must be chosen. Or, equivalently, if both pulses are less intense, they must have a larger duration. Equation (3.13) also relates the chosen length parameters to the required turn-on and-off times of pulse $\Omega_a(z=0,\tau)$:

$$t_{\rm on} = T_b - \frac{2\mu}{B^2} D_2 , \qquad (3.16a)$$

$$t_{\rm off} = T_b - \frac{2\mu}{B^2} D_1 . \qquad (3.16b)$$

This example shows that the pulse duration of the pulse $\Omega_a(z=0,\tau)$, which is $t_{\rm off}-t_{\rm on}=(2\mu/B^2)(D_2-D_1)$, can be chosen arbitrarily short if B is large and the pulse is sufficiently intense.

The two examples above demonstrate that there are many pulse pair combinations that lead to the same spatial excitation profile. If, however, the shape of one of the pulses is specified, then the other is directly determined by $G(z)$. The question arises whether the two pulses Ω_a and Ω_b can have identical envelopes and different amplitudes. Equation (3.12) suggests that in order to excite a localized regime inside the medium, the envelopes should be different.

C. Comparison of the theory with numerical results

This section serves the purpose to compare our analytical results based on adiabaticity with the exact numerical solution of the Liouville-Maxwell equations and to graphically illustrate the spatially and temporally resolved interaction of the fields with the medium. We assume that the medium is initially entirely in its ground state. The relevant parameters are given in the figure captions. The figures on top are the exact data and should be compared directly with those at the bottom that were obtained by graphing the corresponding analytical solutions.

In Figs. 3(a) and 3(b) we display snapshots of the temporal profiles of two pulses taken at various propagation distances. At input ($z=0$) the field Ω_a was chosen to be a simple Gaussian whereas the field Ω_b was practically a square pulse between short turn-on and -off times. It is apparent that both pulses change their shapes significantly as they penetrate the medium. The trailing edge of field Ω_b [right side of graph (b), at $60<\tau<80$] travels with speed c. The pulse Ω_a, however, travels with a reduced velocity. At a certain propagation length $z \approx 2000$ the fast trailing edge of Ω_b has reached the (slow) trailing edge of Ω_a and the pulse Ω_a starts to decay. This decay is accompanied by an increase of the amplitude of field Ω_b. After pulse Ω_a has decayed completely, the final form of Ω_b is practically indistinguishable with the analytical predictions given by Eq. (3.8b).

In Fig. 4 we display the population probability $\rho_{33}(z,\tau)$ as a function of the position z at various times τ. We see that—after its formation—the spatial excitation profile propagates through the medium as well. The spatial distributions for $70<\tau$ becomes ''frozen'' and represents the final excitation function $G(z)$. The data on the bottom correspond to the analytical prediction of Eq. (3.11). The agreement is again very good. The small superimposed oscillations present in

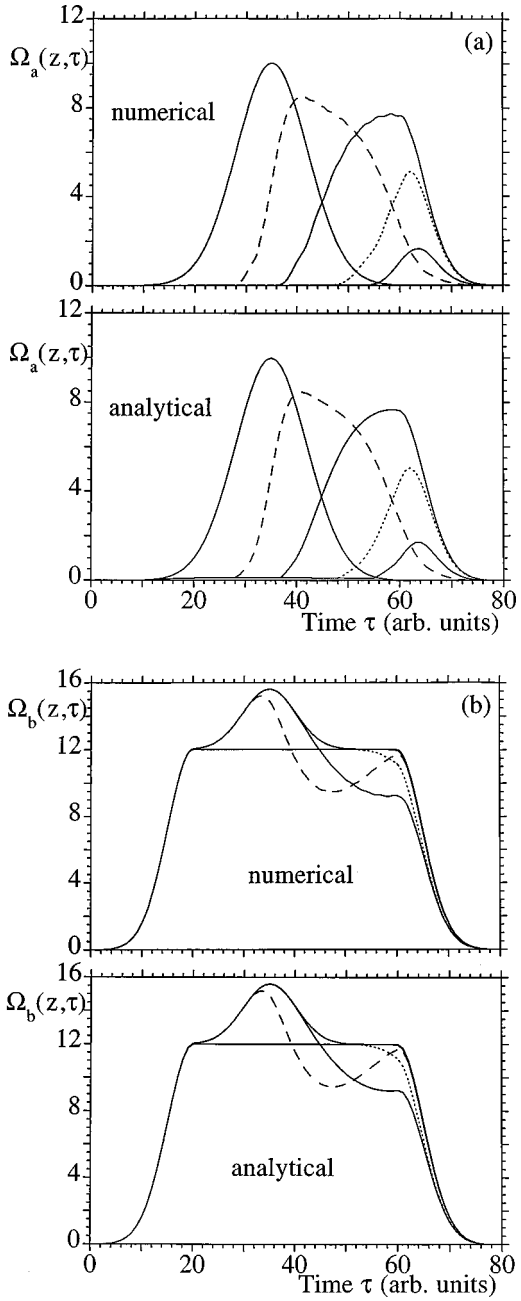

FIG. 3. The temporal evolution of the two laser pulses. The top curve shows the exact data obtained from the numerical solution of Eqs. (2.1) and (2.3); the bottom curve is the prediction according to the analytical formula Eq. (3.7). (a) The temporal profiles of the field Ω_a. These were taken at propagation distances $z=0$, 1000 (dashed line), 2000, 3000 (dotted line), and 3500 (smallest amplitude). The pulse is vanishingly small for propagation distances $z>4000$. (b) The corresponding evolution for the field Ω_b at the same distances as in (a). (The parameters were $\mu_a=\mu_b=1$, $A_{21}=A_{23}=\gamma_{12}=\gamma_{23}=\Gamma=0.05$, $\Delta_a=\Delta_b=0$, $\Omega_a(z=0,\tau)=A\exp\{-0.5[(\tau-35)/7]^2\}$, and $\Omega b(z=0,\tau)=B\exp[-0.5(\tau/\tau p)2]$ *for* $\tau<4\tau_p$; $\Omega_b(z=0,\tau)=B$ *for* $4<\tau/\tau_p<12$ *and* $\Omega_b(z=0,\tau)=B\exp\{-0.5[(\tau-12\tau_p)/\tau_p]^2\}$ *for* $12<\tau/\tau_p$, $A=10$, $B=12$, $\tau_p=5$.)

the exact data (top) could be a manifestation of nonadiabaticity.

In Fig. 5 we display the time integral of the squared Rabi frequency as a function of z for both pulses. Although both

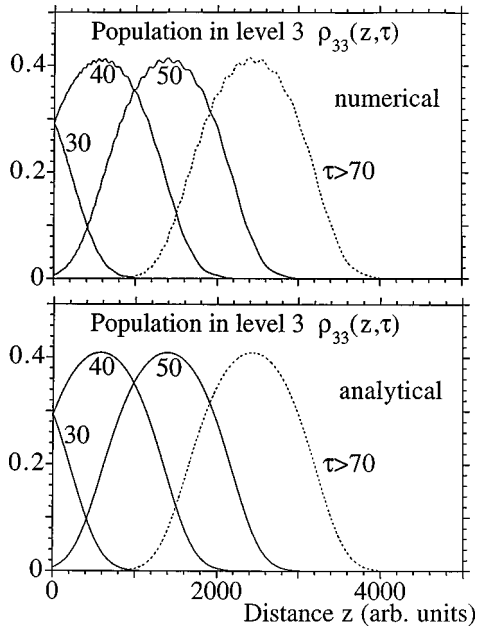

FIG. 4. The spatial evolution of the excitation. The top curve shows the exact data obtained from the numerical solution of Eqs. (2.1) and (2.3); the bottom curve is the prediction according to the analytical formula Eq. (3.11). The spatial distribution of the population $\rho_{33}(z,\tau)$ in the metastable state $|3\rangle$ displayed at times $\tau=30$, 40, 50, and 70. The dashed line corresponds to the final distribution for $\tau>70$ (same parameters as in Fig. 3).

pulses reshape significantly for distances $z<1800$, the individual ''pulse energies'' are conserved. The pulse Ω_a decays to zero and its energy is partially converted to that of pulse Ω_b only for $1400<z<3600$.

In Fig. 6 we show the breakdown of adiabaticity and that of our analytical theory. The same parameters as in the previous figure were chosen but with unequal propagation coefficients which differ by a factor of 3. Compared to the results for $\mu_a=\mu_b$, the temporal front edge of Ω_a steepens. This steepening is accompanied with a breakup of the front edge into several sharp spikes, which can have amplitudes that can exceed the amplitude of the input field Ω_b. None of these features can be predicted by a theory that is based on temporal adiabaticity. For completeness we show in Fig. 6(b) the spatial profile of the final excitation function. We found in

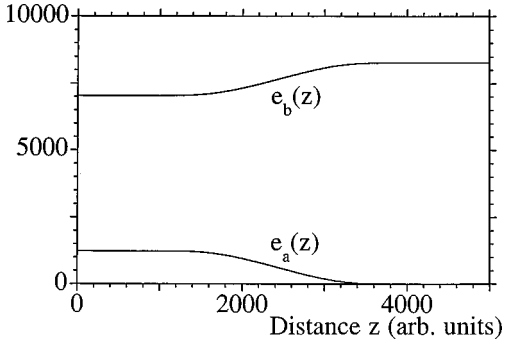

FIG. 5. The time-integrated squared Rabi frequency of the two pulses $e_a(z)\equiv\int d\tau'|\Omega_a(z,\tau')|^2$ and $e_b(z)\equiv\int d\tau'|\Omega_b(z,\tau')|^2$ as a function of the propagation distance z (same parameters as in Fig. 3).

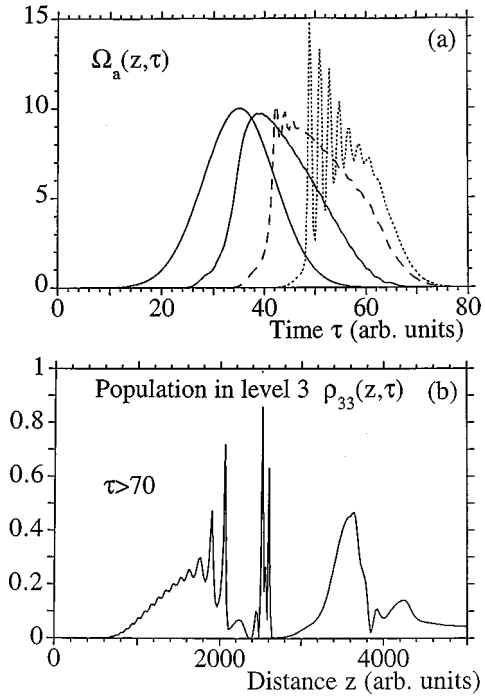

FIG. 6. The breakdown of the analytical theory due to very different propagation coefficients. (a) Temporal profiles of the field Ω_a taken at propagation distances $z=0$, 500, 1000, and 1500 (dotted line). (b) The final spatial distribution of the population $\rho_{33}(z,\tau)$ in the metastable state $|3\rangle$. (With the exception of $\mu_a=1.5$ and $\mu_b=0.5$, all other parameters as in Fig. 3.)

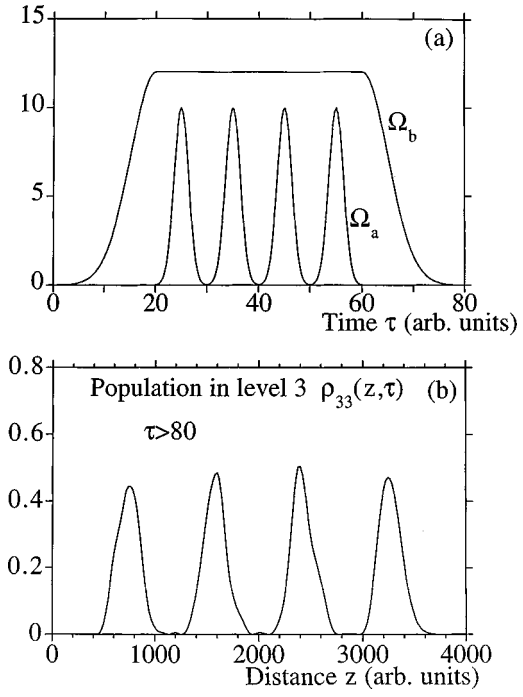

FIG. 7. The generation of a spatially periodic excitation pattern inside the medium produced by a sequence of four input pulses Ω_a. (a) The temporal profiles of the two input fields at $z=0$. (b) The final distribution of population in the metastable state after the pulses have left the medium. (The parameters were $\mu_a=\mu_b=1$, $A_{21}=A_{23}=\gamma_{12}=\gamma_{23}=\Gamma=0.05$, $\Gamma=0.05$, $\Delta_a=\Delta_b=0$, $\Omega_a(z=0,\tau)$ is a sequence of four pulses of the form $\Omega_a(z=0,\tau)=10\exp\{-[(\tau-\tau_c)/2]^2\}$ that are centered at $\tau_c=25$, 35, 45, and 55. The other input field $\Omega_b(z=0,\tau)$ is identical to the one used in Fig. 3.)

most of our numerical simulations that the breakdown of adiabaticity is initiated by a steepening of the temporal front edge.

We conclude this section by demonstrating how a sequence of several laser pulses can be exploited to generate an interesting spatially periodic excitation pattern inside the medium. The field Ω_a was chosen to be a sequence of four Gaussian shaped pulses. The field Ω_b was the same as above. We display the two input pulse shapes in Fig. 7(a) Figure 7(b) shows an interesting spatially periodic pattern of excitation. A study of the optical diffractive properties of such a periodic (index of refraction) pattern and its potential applications will be discussed elsewhere.

IV. PREDICTIONS FOR SPATIAL EXCITATIONS IN A POTASSIUM VAPOR

A possible experimental verification of the excitation of selected spatial domains inside a dielectric material seems to be quite possible in the optical regime of atomic or molecular vapors. In the following we demonstrate how one can obtain spatial excitations for a potassium vapor. This vapor has been used recently to study optically pumped lasers [19], electronic transition moments, and collisional relaxation rates. As this section is designed as a direct guidance for possible experiments, we have used cgs units.

A vapor containing K_2 molecules, where the vapor is contained in a heat-pipe oven, is a possible system to explore three-level physics as appropriate molecular transitions can have very similar oscillator strengths. We consider the situation with the $X\ ^1\Sigma_g^+(v=1,\ J=47)$ level as the ground state $|1\rangle$, the $B\ ^1\Pi_u(v=6,\ J=47)$ level as state $|2\rangle$, and the metastable level $X\ ^1\Sigma_g^+(v=13,\ J=47)$ as state $|3\rangle$. The quantum number v denotes the vibrational level, and the quantum number J denotes the rotational level. The energies of the $|1\rangle$ to $|2\rangle$ and $|3\rangle$ to $|2\rangle$ transitions are 15 690.8 cm^1 and 14 648.7 cm^{-1}, respectively. The dipole moment of the $B\ ^1\Pi_u - X\ ^1\Sigma_g^+$ electronic state transition is 6 debye [20]. The Franck-Condon factors [21] for the $|1\rangle$ to $|2\rangle$ and $|3\rangle$ to $|2\rangle$ transitions are 0.130 and 0.144, respectively [22]. Further, Hönl-London factors decrease the transition intensity by an additional factor of 2. A gas pressure of 800 Pa corresponds to a molecular particle density of $\mathcal{N}=3\times10^{12}$ molecules/cm^3 (most of the pressure is due to atoms). These parameters correspond to the propagation coefficients of μ of approximately $2.7\times10^{10}\ cm^{-1}\ sec^{-1}$ for both transitions. The electronic transitions in K_2 are characterized by the following dissipative decay rates: The total spontaneous emission rate from the upper level is 8.33×10^7 Hz. The dephasing rates due to collisions are not so well known, we estimate them equal and to be $\gamma_{12}=\gamma_{23}=2.4\times10^8$ Hz. The states $|1\rangle$ and $|3\rangle$ are not dipole coupled so one might expect that γ_{13} is much smaller than γ_{12} [23]. The magnitude of the irreversible decay rate of the upper state due to ionization or coupling to other levels denoted by Γ depends on the intensity. A rough estimate yields Γ to be smaller than the other radiative rates.

Both transitions can be resonantly excited

($\lambda_a = 637.3$ nm and $\lambda_b = 682.7$ nm) via radiation from tunable dye lasers, which are in turn pumped by a frequency doubled Nd: YAG (YAG denotes yttrium aluminum garnet) (Spectra Physics) laser. The two pulse envelopes can be varied in temporal length from 3 to 6 nsec.

The temperature of the K_2 gas in the heat pipe is typically around 410 °C, which corresponds to a Doppler width of about 1.7 GHz. The adjacent rovibrational levels are sufficiently far apart that practically no transition becomes dynamically important and we ignore the Doppler effect. The high temperature of the vapor, however, leads to initial thermal populations in state $|3\rangle$ which can be approximately 10%. In the following we assume that the time scale for thermally exciting the state $|3\rangle$ is longer than the laser-medium interaction time and we therefore neglect the possibility of thermal reexcitation. To reflect an initial thermal excitation we have repeated the simulations discussed in Figs. 3–5 for a non zero but spatially constant initial value of $\rho_{33}(z, \tau = 0)$ and assumed that the initial two-photon coherence $\rho_{13}(z, \tau = 0)$ is zero. Basically, a nonzero ρ_{33} has two implications: First, the front edge of the first injected pulse Ω_b that is resonant with the ''nonempty'' 3-2 transition steepens and is being absorbed by the medium. The energy of the pulse Ω_b decreases therefore as the pulse propagates even before pulse Ω_a begins to decay. However, if both pulses have comparable Rabi frequencies, the relative speed at which the location of the front edge moves towards the center of the pulse is comparable to the relative speed with which the trailing edge Ω_b approaches the slow pulse Ω_a. As the final remaining excitation function is determined only by the interaction of the pulses with the medium at the trailing end, the absorption of the front edge of the pulse Ω_b is not so crucial.

Second, only the fraction $\rho_{11}(z, \tau = 0)$ of the molecules can initially satisfy the trapped state condition for counterintuitively injected pulses. In other words, one can assume that the number density $\mathcal{N}$ (and therefore the propagation constant μ) is effectively reduced by the factor $\rho_{11}(z, \tau = 0)$, $\mu_{\text{eff}} = \mu \rho_{11}$. This leads to a faster propagation velocity of pulse Ω_a and therefore to a broader final excitation distribution. All of our simulations with various values for $\rho_{11}(z, \tau = 0)$ were in good agreement with the analytical estimates discussed in Sec. III B with respect to the location and width of the final excitation function if we used an effective μ_{eff}.

In Fig. 8 we show an example for a pair of Gaussian input pulses. Ω_a (Ω_b) has an intensity width [full width at half maximum (FWHM)] of 3 nsec (6 nsec), a Rabi frequency of 0.022 cm^{-1} (0.026 cm^{-1}). In Fig. 8(b) we display the final population in level $X\ ^1\Sigma_g^+(v = 13,\ J = 47)$ as a function of the distance. In order to probe the final excitation distribution, one can inject an additional laser beam at 682.7 nm to recall the spatial excitation as outlined in Ref. [14]. This recall field, however, should not be delayed by more than the two-photon coherence decay time $(\gamma_{13})^{-1}$. More directly, one can probe the medium using a tunable dye laser and analyzing the associated laser-induced fluorescence. The latter technique would require a disk-type heat-pipe design which allows for the injection of probe laser beams perpendicular to the main propagation direction.

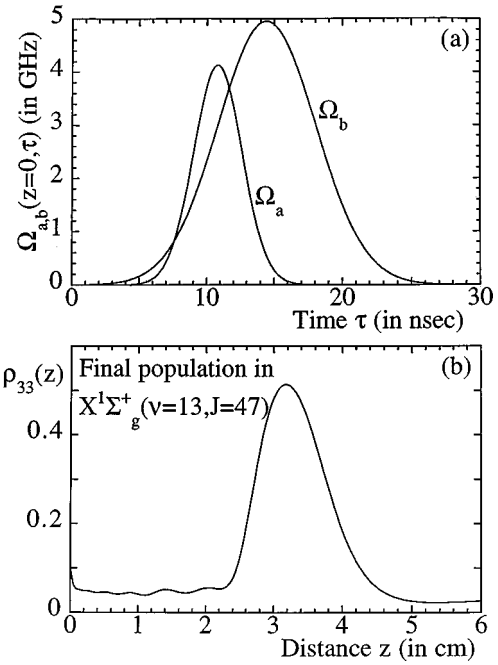

FIG. 8. The generation of a spatial excitation pattern inside a vapor of K_2 molecules. (a) The temporal profiles of the two input fields at $z = 0$. (b) The final distribution of population in the metastable state $X\ ^1\Sigma_g^+(v = 13,\ J = 47)$ after the pulses have left the medium. After 5 cm the final excitation is established and the pulse Ω_a has decayed. (The parameters [see Eq. (2.1)] were chosen to match as closely as possible experimentally achievable conditions: $\mu_a = \mu_b = 2.73 \times 10^{10}\ \text{cm}^{-1}\ \text{sec}^{-1}$, $\Gamma = 100$ MHz, $\Delta_a = 10$ MHz, $\Delta_b = 10$ MHz, $A_{21} = 11$ MHz, $A_{22} = 12$ MHz, $\gamma_{12} = \gamma_{23} = 12$ MHz, $\gamma_{13} = 1.2$ MHz, $\Omega_a(z = 0, \tau) = A\ \exp[-((\tau - 10.8\ \text{nsec})/(1.67\tau_p))^2]$; $\Omega_b(z = 0, \tau) = B\ \exp\{-[(\tau - 14.4\ \text{nsec})/(3.34\tau_p)]^2\}$, $\tau_p = 3$ nsec, $A = 4.13$ GHz, $B = 4.96$ GHz).

V. DISCUSSION

In order to obtain fully analytical results, the description was restricted to the case of equal oscillator strengths between the relevant transitions. The larger the ratio between the oscillator strengths, the shorter is the propagation distance after which effects due to nonadiabaticity become important. In most of our numerical simulations we found that the breakdown of adiabaticity occurs due to a steepening of the temporal front edge of pulse Ω_a. This steepening is then accompanied with a breakup of the front edge into several sharp spikes, which can have an amplitude that can exceed the amplitude of the input field Ω_b by an order of magnitude. Another measure for the magnitude of effects due to nonadiabaticity is the quantity $\Omega_a^2/\mu_a + \Omega_b^2/\mu_b$ which should not change as a function of space if the dynamics is adiabatic and governed by Eqs. (3.3). Another source for nonadiabaticity is the collisional broadening between the two-photon resonant ground and metastable states. As the excitation process relies on the two-photon coherence, this type of relaxation has the largest impact on the dynamics. There are still several aspects of a real laboratory experiment which were not taken into account in our model; these include possibly chaotic multimode temporal laser envelopes, transverse propagation effects, quick rethermalization during the interaction, the possible interaction of more than three molecular states with the field, and possible shifts in the lasers' polar-

ization direction due to spontaneous emission or collisions. Experimental data would shine some light on the relative importance of these effects.

Let us now complete this discussion with a quite speculative outlook at possible applications for the proposed excitation process. In general the key parameter to describe the optical properties of any material is the index of refraction. To generate and to control this index is the goal of many manufacturing processes for optical devices such as optical fibers, optical instruments such as lenses, or even gases. The control of the optical propagation properties of gases is also of interest in adaptive optics. It is typical for most manufacturing processes, however, that once an index of refraction has been imprinted on a medium, a further modification of the index is practically impossible without destroying the material. This can be costly. In most cases spatially irreversible structures and a permanent index of refraction are quite desirable. However, one could imagine situations in which it is advantageous to have a material in which the index of refraction can be easily adjusted to specific and changing optical requirements.

The index of refraction of any dielectric optical material depends directly on the structure of its quantum-mechanical energies and the dipole moments. A material in a metastable state can have completely different absorptive and dispersive properties than the same material in its ground state. The index of refraction can be controlled using our process to ''manufacture'' the degree of excitation of a material as a function of the position in a desired way. As an example we have shown that a sequence of several pulses Ω_a at input generates a spatially modulated periodic index of refraction leading to quite interesting refractive properties. The spatial wavelength of this periodic pattern can be controlled directly by the repetition rate of the input laser pulses. The lifetime of this spatial pattern is given by the lifetime of the metastable state and not by the (typically shorter) phase relaxation time. In general, metastable states can have lifetimes that can range from nanoseconds to hours, depending on the specific state.

ACKNOWLEDGMENTS

We would like to thank J. H. Eberly, A. Merriam, and Q. Su for useful discussions, and M. M. Jacobs for his help with the numerical work. This work was supported by the NSF under Grant No. PHY-9631245. We acknowledge partial support by the Cottrel Science Award program of Research Corporation and by Illinois State University. J.R.C. would like to thank the ISU-Honors undergraduate program for support of her research work.

[1] See, e.g., U. Gaubatz, P. Rudecki, S. Schiemann, and K. Bergmann, J. Chem. Phys. **92**, 5363 (1990).

[2] K.-J. Boller, A. Imamoglu, and S. E. Harris, Phys. Rev. Lett. **66**, 2593 (1991); J. E. Field, K. H. Hahn, and S. E. Harris, *ibid.* **67**, 3062 (1991). For a review, see S. E. Harris, Phys. Today **50**(7), 36 (1997), and references therein.

[3] F. T. Hioe and R. Grobe, Phys. Rev. Lett. **73**, 2559 (1994); J. H. Eberly, Quantum Semiclassic. Opt. **7**, 373 (1995).

[4] G. Vemuri, G. S. Agarwal, and K. V. Vasavada, Phys. Rev. Lett. **79**, 3889 (1997).

[5] K. M. Paul, J. R. Csesznegi, and R. Grobe, Laser Phys. **7**, 884 (1997).

[6] R. Grobe, F. T. Hioe, and J. H. Eberly, Phys. Rev. Lett. **73**, 3183 (1994).

[7] For recent work which discusses the adiabaton pulse propagation regime, see, e.g., I. E. Mazets and B. G. Matisov, Phys. Rev. A **52**, 4941 (1995); R. Grobe and J. H. Eberly, Laser Phys. **5**, 542 (1995); M. Fleischhauer and A. Manka, Phys. Rev. A **54**, 794 (1996); I. E. Mazets, *ibid.* **54**, 3539 (1996); J. H. Eberly, A. Rahman, and R. Grobe, Laser Phys. **6**, 69 (1996); R. Grobe, Acta Phys. Pol. A **93**, 87 (1998).

[8] A. Kasapi, M. Jain, G. Y. Yin, and S. E. Harris, Phys. Rev. Lett. **74**, 2447 (1995).

[9] M. O. Scully, Phys. Rev. Lett. **55**, 2802 (1985); **67**, 1855 (1991).

[10] For a review on phaseonium, see, e.g., M. O. Scully, Phys. Rep. **219**, 191 (1992); Quantum Opt. **6**, 201 (1994).

[11] J. H. Eberly, A. Rahman, and R. Grobe, Phys. Rev. Lett. **76**, 3687 (1996).

[12] G. Vemuri, K. V. Vasada, and G. S. Agarwal, Phys. Rev. A **54**, 3394 (1996).

[13] T. Nakajima, Opt. Commun. **136/3-4**, 273 (1997).

[14] J. R. Csesznegi and R. Grobe, Phys. Rev. Lett. **79**, 3162 (1997).

[15] B. J. Herman, J. H. Eberly, and M. G. Raymer, Phys. Rev. A **39**, 3447 (1989); and P. W. Milonni and J. H. Eberly, J. Chem. Phys. **68**, 1602 (1978).

[16] G. Alzetta, A. Gozzini, L. Moi, and G. Orriols, Nuovo Cimento B **36**, 5 (1976); R. M. Whitle and C. R. Stroud, Jr., Phys. Rev. A **14**, 1498 (1976).

[17] For theoretical work on the principle of counterintuitivity see J. Oreg, F. T. Hioe, and J. H. Eberly, Phys. Rev. A **29**, 690 (1984); C. E. Carroll and F. T. Hioe, *ibid.* **42**, 1522 (1990).

[18] J. R. Kuklinski, U. Gaubatz, F. T. Hioe, and K. Bergmann, Phys. Rev. A **40**, R6741 (1989).

[19] See, e.g., B. K. Clark and A. D. Glueck, Quantum Opt. **6**, 341 (1994), and references therein.

[20] W. J. Tango and R. N. Zare, J. Chem. Phys. **53**, 3094 (1970).

[21] G. Herzberg, *Spectra of Diatomic Molecules* (Van Nostrand Reinhold, New York, 1950).

[22] B. K. Clark, K. A. Page, and C. A. Stack, Chem. Phys. **163**, 371 (1992); B. K. Clark, J. M. Standard, Z. J. Smolinski, D. R. Ripp, and J. R. Flemming, *ibid.* **213**, 229 (1996).

[23] For measurement techniques of two-photon dephasing times, see A. Kasapi, G. Y. Yin, M. Jain, and S. E. Harris, Phys. Rev. A **53**, 4547 (1996).